HHS Public Access

Author manuscript

Mol Carcinog. Author manuscript; available in PMC 2015 March 23.

Published in final edited form as:

Mol Carcinog. 2015 January ; 54(1): 9–23. doi:10.1002/mc.22070.

Inhibition of FAK and VEGFR-3 Binding Decreases Tumorigenicity in Neuroblastoma

Jerry E. Stewart[1], **Xiaojie Ma**[2], **Michael Megison**[1], **Hugh Nabers**[1], **William G. Cance**[3], **Elena V. Kurenova**[3], and **Elizabeth A. Beierle**[1,*]

[1]University of Alabama, Birmingham, 1600 7th Ave. S., Lowder Building, Room 300, Birmingham, Alabama

[2]University of Florida, 1600 Archer Road, Gainesville, Florida

[3]Roswell Park Cancer Institute, Elm and Carlton Streets, Buffalo, New York

Abstract

Neuroblastoma is the most common extracranial solid tumor of childhood and is responsible for over 15% of pediatric cancer deaths. Focal adhesion kinase (FAK) is a nonreceptor tyrosine kinase that is important in many facets of tumor development and progression. Vascular endothelial growth factor receptor-3 (VEGFR-3), another tyrosine kinase, has also been found to be important in the development of many human tumors including neuroblastoma. Recent reports have found that FAK and VEGFR-3 interact, and we have previously shown that both of these kinases interact in neuroblastoma. We have hypothesized that interruption of the FAK–VEGFR-3 interaction would lead to decreased neuroblastoma cell survival. In the current study, we examined the effects of a small molecule, chloropyramine hydrochloride (C4), designed to disrupt the FAK–VEGFR-3 interaction, upon cellular attachment, migration, and survival in two human neuroblastoma cell lines. We also utilized a murine xenograft model to study the impact of C4 upon tumor growth. In these studies, we showed that disruption of the FAK–VEGFR-3 interaction led to decreased cellular attachment, migration, and survival in vitro. In addition, treatment of murine xenografts with chloropyramine hydrochloride decreased neuroblastoma xenograft growth. Further, this molecule acted synergistically with standard chemotherapy to further decrease neuroblastoma xenograft growth. The findings from this current study help to further our understanding of the regulation of neuroblastoma tumorigenesis, and may provide novel therapeutic strategies and targets for neuroblastoma and other solid tumors of childhood.

Keywords

FAK; FLT-4; SK-N-AS; SK-N-BE(2); C4

*Correspondence to: University of Alabama, Birmingham, 1600 7th Ave. South, Lowder Building, Room 300, Birmingham, AL 35233..

Conflict of interest: None.

SUPPORTING INFORMATION

Additional supporting information may be found in the online version of this article at the publisher's web-site.

INTRODUCTION

Neuroblastoma is the most common extracranial solid tumor of childhood. This tumor arises from neural crest cells and often presents with advanced stage disease. Despite significant advances in both medical and surgical pediatric oncologic care, this tumor continues to carry a dismal prognosis, especially for children with metastatic or advanced disease, with a survival of <30% [1]. Clearly, novel therapies will need to be developed to improve the outcomes for children with this disease.

Focal adhesion kinase (FAK) is a 125 kDa non-receptor protein tyrosine kinase that has been shown to be important in the tumorigenesis of a number of human tumors. FAK has been shown to be involved in tumor cell proliferation, motility, survival, and apoptosis [2–5]. The inhibition of FAK through a number of different means has been shown to affect tumorigenesis. FAK inhibition with RNAi, resulted in decreased motility in glioblastoma cells [6]. In other studies, inhibition of FAK with antisense oligonucleo-tides or a dominant-negative FAK protein resulted in decreased melanoma and breast cancer cell growth [7–10]. Small molecule inhibition of FAK has resulted in decreased growth and increased apoptosis in ovarian cancer cells [11] and glioma cells [12].

Previous studies have shown that FAK mRNA and protein were associated with aggressive neuroblastomas [13] and that FAK inhibition through a number of different mechanisms resulted in decreased neuroblastoma survival [14–16].

Vascular endothelial growth factor receptor-3 (VEGFR-3) is a receptor tyrosine kinase that is modulated by its ligands vascular endothelial growth factors C and D [17]. VEGFR-3 is important in normal lymphangiogenesis and has recently been shown to play a role in tumor lymphangiogenesis in a number of human tumors [18–20]. It was demonstrated that overexpression of VEGFR-3 leads to aggressive tumor growth [21] and inhibition of VEGFR-3 with competing antibodies has been shown to decrease the growth of a number of human tumor xenografts [22]. We have shown that VEGFR-3 mRNA was differentially expressed in human neuroblastoma cells [23,24]. Other authors have shown that the VEGFR-3 ligand, VEGF-C was expressed in some neuroblastoma cell lines and that lymphangiogenesis was involved in neuroblastoma tumor formation [25]. A recent report from Rossler and colleagues demonstrated decreased neuroblastoma xenograft tumor growth following treatment with the VEGFR1-3 inhibitor, AG-013736 [26].

There have been recent reports describing the interaction between FAK and VEGFR-3, and showing that disruption of this interaction with homologous peptides or small molecules resulted in decreased tumor cell survival [27–29]. We have demonstrated that FAK and VEGFR-3 interact in human neuroblastoma cell lines [29], and now hypothesize that inhibition of this interaction would result in decreased neuroblastoma tumorigenicity. The data from the current study showed that disruption of the FAK–VEGFR-3 interaction with chloropyramine hydro-chloride (C4) resulted in decreased neuroblastoma attachment, invasion and survival. In addition, C4 treatment of neuroblastoma xenografts led to decreased tumor growth, and finally, combining C4 and doxorubicin had a synergistic effect upon neuroblastoma xenograft growth. These data demonstrated that VEGFR-3 plays a role

in tumor progression, through its interaction with FAK, which was independent of its pro-lymphangiogenic activities.

MATERIALS AND METHODS

Cells and Cell Culture

Human neuroblastoma cells lines, SK-N-AS (CRL-2137, American Type Culture Collection, ATCC, Manassas, VA) and SK-N-BE(2) (CRL-2271, ATCC) were maintained as follows: SK-N-AS in Dulbecco's modified Eagle's medium with 4 mM L-glutamine, 0.1 mM nonessential amino acids, 1 mg/mL penicillin and 1 mg/mL streptomycin, and 10% fetal bovine serum (FBS), and SK-N-BE(2) in a 1:1 mixture of MEM and F12 medium with 1 mg/mL penicillin, 1 mg/mL streptomycin, and 10% FBS.

Antibodies and Reagents

Antibodies used for Western blotting and immunohistochemistry were as follows. Phospho-specific VEGFR-3 antibody (CB5793, rabbit polyclonal) was from Cell Applications (Cell Applications, Inc., San Diego, CA). Antibodies for VEGFR-3 were either from Millipore (MAB3757, clone 9D9F9, EMD Millipore, Billerica, MA), Santa Cruz (C-20, sc-321, rabbit polyclonal, Santa Cruz Biotechnology, Inc., Santa Cruz, CA) or Abcam (ab27278, rabbit polyclonal, Abcam, Cambridge, MA). Antibody for cleaved poly (ADP-ribose) polymerase (PARP) was from Cell Signaling (9542s, rabbit polyclonal, Cell Signaling Technology, Inc., Danvers, MA). Monoclonal anti-FAK (4.47) and rabbit polyclonal anti-phospho-FAK (Y397) antibodies were obtained from EMD Millipore (05–537), and Invitrogen (44624G, Invitrogen Corp., Carlsbad, CA), respectively. GAPDH antibody was from Fitzgerald (10R-1178, Fitzgerald Industries International, Acton, MA) and β-actin antibody was from Santa Cruz.

Antibodies used for immunofluorescence were as listed: primary antibody to VEGFR-3 was a rabbit polyclonal (C-20, 1:1000 dilution, Santa Cruz), and to FAK (4.47) was a mouse monoclonal (05–537, 1:1000 dilution, EMD Millipore). Secondary antibodies for immunofluorescence were from Invitrogen and included goat anti-rabbit Alexa Fluor 488 (A-11008, 1:200 dilution) and goat anti-mouse Alexa Fluor 594 (A-21044, 1:200 dilution).

Chloropyramine hydrochloride (C4) was obtained from Sigma–Aldrich (C1915, Sigma–Aldrich, St. Louis, MO) for in vitro studies, and as a sterile solution for injection (20 mg/mL, EGIS, Hungary) for in vivo experiments.

Immunofluorescence

Cells were plated on glass chamber slides and allowed to attach for 24 h. After 24 h of C4 treatment, they were fixed with 3% paraformaldehyde. Cells were permeablized with 0.15% Triton X-100 and the first primary antibody (anti-VEGFR-3, C-20, Santa Cruz) was added and incubated at room temperature (RT) for 1 h followed by the addition of the second primary antibody (anti-FAK, 4.47, Millipore) that was also incubated for 1 h at RT. The Alexa Fluor 488 secondary antibody was added for 45 min at RT. After washing, the second secondary antibody, Alexa Fluor 594, was added and incubated as above. Prolong Gold

antifade reagent with DAPI (P36931, Invitrogen) was used for mounting. Imaging was performed with a Zeiss LSM 710 Confocal Scanning Microscope with Zen 2008 software (Carl Zeiss MicroImaging, LLC, Thornwood, NY) using a 63 objective with a zoom of 0.9. Analysis of the images and detection of confocal overlap was accomplished utilizing the MetaMorph® Microscopy Image Analysis Software (Ver. 7.6, Analytical Technologies, Molecular Devices, Sunnyvale, CA).

Manders' overlap coefficients were calculated for each of the treatment groups [30]. Manders' M1 and M2 coefficients have a value between 0 and 1 (0 = no overlap; 1 = perfect overlap) and provide the proportion of the overlap of each channel with the other. The M1 and M2 coefficients were calculated as follow: M1 (red) = the sum of the intensities of red pixels that had a green component divided by the total sum of red intensities; and M2 (green) = the sum of the intensities of green pixels that had a red component divided by the total sum green intensities.

Cell Viability and Apoptosis

Equal numbers of cells were plated and allowed to attach for 24 h. Cells were treated with C4 in varying concentrations. Cellular viability was measured using alamarBlue® assay. In brief, cells were plated 1.5×10^3 cells per well on 96-well culture plates and allowed to attach. Following treatment, 10 μL of alamarBlue® dye (Invitrogen) was added to 200 μL of cell medium. After 4–6 h, the absorbance at 595 nm was measured using a kinetic microplate reader (BioTek Gen5, BioTek Instruments, Winooski, VT).

Apoptosis was detected by immunoblotting for PARP cleavage. Cells were treated with C4, lysates were collected, and immunoblotting for cleaved PARP was performed. Bands were detected by chemiluminescence and β-actin served as an internal control.

Cell Detachment

Equal numbers of cells were plated and allowed to attach for 24 h. The cells were then treated with C4. After 48 h of treatment, detached and adherent cells were collected separately and counted with a hemacytometer. The percentage of detached cells was determined for each experiment (detached/attached + detached × 100) and reported as fold change in detached cells.

Cell Migration

Twelve-well culture plates with 8 mm micropore inserts were utilized for cell migration assays. The bottom side of the insert was coated with collagen (10 mg/mL, 50 μL for 4 h at 37°C). Cells were treated with C4 and 5×10^3 cells were placed into the upper well. Cells were cultured for 24 h and allowed to migrate through the micropore insert. The cells on the inserts were fixed with 3% paraformaldehyde, stained with crystal violet (0.05%), digested with crystal violet extraction buffer (45% ethanol, 2% propanol, 2% methanol, and 1% acetic acid) and absorbance measured at 595 nm using a kinetic microplate reader (BioTek Gen5). Migration was reported as change in cells migrated as measured by change in absorbance.

Immunoblotting

Western blots were performed as previously described [29]. Briefly, cells were treated with the agent under study, then lysed on ice for 30 min in a buffer containing 50 mM Tris–HCL, (pH 7.5), 150 mM NaCl, 1% Triton-X, 0.5% sodium deoxycholate (NaDOC), 0.1% SDS, 5 mM EDTA, 50 mM NaF, 1 mM $NaVO_3$, 10% glycerol, and protease inhibitors: 10 μg/mL leupeptin, 10 μg/mL PMSF and 1 μg/mL aprotinin. The lysates were cleared by centrifugation at 10 000 rpm for 30 min at 4°C. Protein concentrations were determined using a Bio-Rad kit (Bio-Rad, Hercules, CA) and proteins were separated by electrophoresis on sodium dodecyl sulfate–polyacrylamide gel electrophoresis (SDS–PAGE) gels. Antibodies were used according to manufacturer's recommended conditions. Molecular weight markers were used to confirm the expected size of the target proteins. Immunoblots were developed with chemiluminescence Amersham ECL Western blotting detection reagents (GE Healthcare Biosciences, Piscataway, NJ). Blots were stripped with stripping solution (Bio-Rad) at 37°C for 15 min and then reprobed with selected antibodies. Immunoblotting with antibody to β-actin or GAPDH provided an internal control for equal protein loading.

Tumor Growth In Vivo

Six-week-old female nude mice (athymic Nude-*Foxn1*^{nu}) were purchased from Harlan Laboratories, Inc. (Indianapolis, IN). The mice were maintained in a SPF animal facility approved by the American Association of Accreditation of Laboratory Animal Care and in accordance with current regulations and standards of the U.S. Department of Agriculture. Animals were housed with standard 12 h light/dark cycles and allowed chow and water *ad libitum*. All experiments were performed after obtaining protocol approval by the University of Florida Animal Care and Use Committee (200801260), and in compliance with the NIH animal use guidelines. Human neuroblastoma cells [SK-N-AS (AS) or SK-N-BE(2)], 2×10^6 (200 μL), in Matrigel™ (BD Biosciences, San Jose, CA) were injected subcutaneously into the right flank. The flank xenograft model was chosen for its ease. This model, although it may not be the most biologically faithful to the condition of neuroblastoma, allows for the study of human tumor cells and close monitoring of tumor growth with little discomfort to the animal. In contrast, following tumor progression in a genetically engineered murine or a bioluminescence models, requires invasive measures and repeated administration of anesthesia for the animals. When the tumors reached palpable size (100 mm^3), animals were treated daily with intraperitoneal injections of control vehicle (sterile normal saline) or C4 (60 mg/kg/day). Previous experiments with various doses and dosing schedules of the compound proved this to be the optimal, nontoxic dose [28].

The second set of experiments tested the combination of C4 with doxorubicin. SK-N-AS and SK-N-BE(2) neuroblastoma flank xenografts were established in 6-wk-old athymic nude mice as above. Doxorubicin was chosen as it is a standard chemotherapeutic agent for neuroblastoma. Once the tumors measured approximately 100 mm^3, the animals (8 mice/group) were randomized to receive either intraperitoneal injections of vehicle (sterile normal saline) daily, C4 (40 mg/kg/day), doxorubicin (1 mg/kg/every 3 days), or C4 (40 mg/kg/day) plus doxorubicin (1 mg/kg/ every 3 days).

Tumors were measured twice weekly with a caliper and tumor volume in mm^3 was calculated using the standard formula [(width)^2 × length]/2, where width is the smaller diameter. Animals were sacrificed after 4 wk or when tumor size reached protocol end point. The tumors were excised, weighed, and preserved for immunohistochemistry.

Immunohistochemistry

Formalin-fixed, paraffin-embedded tumor blocks were obtained from the xenografts at the completion of the experiment, and 8 μm sections were cut. The slides were baked for 1 h at 70°C, deparaffinized, rehydrated, and steamed. The sections were then quenched with 3% hydrogen peroxide and blocked with PBS-blocking buffer. The primary antibodies, monoclonal anti-FAK 4.47 (1:100, 05-537, EMD Millipore), rabbit polyclonal anti-phospho-FAK (Y397) (1:200, 4624G, Invitrogen), rabbit polyclonal anti-phospho-VEGFR-3 (1:200, CB5793, Cell Applications) or rabbit polyclonal anti-VEGFR-3 (1:200, ab27278, Abcam) were added and incubated overnight at 4°C. After washing with PBS, the secondary antibodies were added 1:250 dilution (Jackson ImmunoResearch Laboratories, Inc., West Grove, PA) for 1 h at 22°C. For Ki67 staining, the primary anti-Ki67 antibody (ab15580, Abcam) was added 1:200 dilution and incubated overnight at 4°C. After washing with PBS, the donkey anti-rabbit secondary antibody was added 1:400 dilution (Jackson ImmunoResearch Laboratories, Inc., West Grove, PA) for 1 h at 22°C. The staining reactions were developed with VECTASTAIN Elite ABC kit (PK-6100, Vector Laboratories, Burlingame, CA), TSA™ (biotin tyramide reagent, 1:400, PerkinElmer, Inc., Waltham, MA) and DAB (Metal Enhanced DAB Substrate, Thermo Fisher Scientific, Rockford, IL). Slides were counterstained with hematoxylin. Negative controls [mouse IgG (1 μg/ mL, Invitrogen) or rabbit IgG (1 μg/mL, EMD Millipore)] were included with each run. Quantification of Ki67 staining (proliferative activity) was reported as percent positive staining cells per total number of cells.

Data Analysis

Experiments were repeated at least in triplicate, and data were reported as mean ± standard error of the mean. Densitometry of immunoblots was performed utilizing Scion Image Program (http://www.nist.gov/lispix/imlab/prelim/dnld.html). Quantification of Ki67 staining was completed using the NIH ImageJ software (http://rsbweb.nih.gov/ij/download.html). An ANOVA or Student's *t*-test was used as appropriate to compare data between groups. Statistical significance was determined at $P \leq 0.05$.

RESULTS

The Small Molecule C4 Interrupted the FAK–VEGFR-3 Interaction

We have previously shown that FAK and VEGFR-3 interact in neuroblastoma and that a peptide from the VEGFR-3 binding site could disrupt this interaction [29]. Previous data in breast cancer cell lines showed that the small molecule, chloropyramine hydrochlo-ride (C4) would disrupt FAK-VEGFR-3 binding [28]. We wished to determine whether treatment with C4 would disrupt the interaction between FAK and VEGFR-3 in neuroblastoma cells. SK-N-AS and SK-NBE(2) neuroblastoma cells were stained for both FAK and VEGFR-3 and confocal microscopy was utilized to determine the degree of colocalization between the

two proteins (Figure 1A–D). Manders' overlap coefficients were calculated for each of the treatment groups (Figure 1E) [30]. Following treatment with C4, there was a decline in the colocalization of FAK and VEGFR-3 in the cell lines (Figure 1B,D), with a significant decrease in the Manders' overlap coefficients for both of the cell lines following C4 treatment (Figure 1E). C4 treatment also resulted in a loss of FAK from the focal adhesions (Figure 1B,D).

C4 Led to Decreased Neuroblastoma Cell Viability, Apoptosis, Detachment, and Decreased Migration

Since it has been shown that the FAK–VEGFR-3 interaction increased tumor cell survival [28,29], we next examined whether C4 disruption of this interaction would affect neuroblastoma cellular viability. SKN-AS and SK-N-BE(2) neuroblastoma cells were treated with varying concentrations of C4 for 24 h and cellular viability was measured. Both cell lines demonstrated a decrease in survival that was signifi-cant at 100 μM concentration (Figure 2A). The calculated LC_{50} for C4 was similar in the two cell lines at 170 μM in the SK-N-AS cell line and 144 mM in the SK-N-BE(2) cell line.

The next experiment was to determine whether the decreased cellular viability in the neuroblastoma cell lines seen following C4 treatment was due to apoptosis. The SK-N-AS and SK-N-BE(2) neuroblastoma cell lines were treated with C4 at increasing concentrations for 24 h and immunoblotting was used to determine the presence of cleaved PARP, an indicator of cellular apoptosis. There was an increase in cleaved PARP in both cell lines. In the SK-N-BE(2) cells, the increase was obvious after treatment with 150 μM of C4 (Figure 2B, *blot and lower left graph*). In the SK-N-AS cell line, the increase in cleaved PARP was noted after treatment with C4 at a concentration of 100 μM (Figure 2B, *blot and lower right graph*).

After noting the changes in viability, we wished to determine if disruption of the FAK–VEGFR-3 interaction would cause other phenotypic changes. The tumorigenicity and metastatic potential of cancer cells depends upon the ability to avoid apoptosis associated with loss of cellular adhesion (anoikis) [31,32]. In addition, it has long been recognized that the most aggressive cancer cells migrate through extracellular matrices and invade surrounding tissues. Therefore, we investigated the effects of C4 upon cellular attachment and migration. The SK-N-AS and SK-N-BE(2) cells were treated with increasing concentrations of C4 and cellular detachment measured. C4 treatment at concentrations of 50 μM and higher caused a significant increase in detachment in both the SK-N-AS (1 vs. 3.05 ± 0.6, $P = 0.04$, 0 vs. 50 μM C4) and the SK-N-BE(2) (1 vs. 1.4 ± 0.1, $P = 0.02$, 0 vs. 50 μM C4) cell lines (Figure 2C). Next, cellular migration was evaluated after treating both neuroblastoma cell lines with increasing concentrations of C4. Migration was also significantly inhibited in both cell lines with C4 treatment (Figure 2D). After treatment with 50 μM of C4, migration decreased to 0.61 in the SK-N-AS cells and to 0.57 in the SK-N-BE(2) cells (Figure 2D). Changes in detachment and migration were noted in both cell lines at concentrations of C4 well below the calculated LC_{50}. These data demonstrated that C4 treatment resulted in signifi-cant changes in the phenotypes in these neuroblastoma cell lines, and that these changes were independent of cell death.

Kinase Phosphorylation

To define a potential mechanism for the phenotypic changes seen in the neuroblastoma cells following C4 treatment, we investigated the biochemical effects of C4 in the SK-N-AS and SK-N-BE(2) cell lines. Cells were treated with C4 at 100 μM for 24 h and were evaluated for phosphorylation of VEGFR-3 and FAK with immunoblotting. Treatment of these cell lines resulted in no change in the phosphorylation of Y1063/1068 VEGFR-3 or VEGFR-3 expression (Figure 3A,B, *blots and graphs*), but did decrease the phosphorylation of Y397 FAK (Figure 3A,B, *blots and graphs*).

Neuroblastoma Tumor Growth In Vivo

We utilized a subcutaneous xenograft tumor model to examine the effects of C4 treatment upon neuroblastoma in vivo tumor growth. For the first experiment, 6-wk-old female athymic nude mice were injected with SK-N-AS or SK-N-BE(2) cells. Once the tumors were palpable, approximately 100 mm^3 (Day 0), the animals were treated daily with intraperitoneal injections of vehicle (sterile normal saline, $n = 10$) or C4 (60 mg/kg/dose, $n = 10$). In the SK-N-AS animals, C4 did not significantly affect xenograft growth (Figure 4A). Conversely, in the SK-N-BE(2) animals, tumor growth was significantly decreased by C4 treatment (Figure 4B). Tumor weights were also examined. In the SK-N-AS xenografts, there was a decrease in the final tumor weights in the animals treated with C4, but this did not reach statistical significance (1.14 ± 0.38 g vs. 0.57 ± 0.011 g, control vs. C4, $P = 0.08$) (Figure 4C). In the SK-N-BE(2) animals, the tumor weights followed the trend of the tumor growth curve, and there was a significant decrease in tumor weights in the C4 treated animals (1.02 ± 0.3 g vs. 0.39 ± 0.1 g, control vs. C4, $P = 0.04$) (Figure 4D).

In the in vitro studies, C4 resulted in a decrease in FAK phosphorylation. We performed immunohisto-chemical staining on both the SK-N-AS and SK-N-BE (2) murine neuroblastoma xenografts, with representative photomicrographs presented in Figure 5A and B. Immunohistochemical staining revealed that in the xenografts, from both cell lines, treated with C4, staining for phosphorylated FAK was decreased when compared to those treated with saline. There was not an appreciable difference in VEGFR-3 staining in either the SK-N-AS or SK-N-BE(2) xenografts (data not shown).

Since FAK is involved in tumor cell proliferation, we wished to see if proliferation was affected by C4 treatment in vivo. Cellular proliferation may be detected by Ki-67 staining, and this was completed on the tumor xenograft specimens. Formalin-fixed, paraffin-embedded tumor xenografts from both SK-NAS and SK-N-BE(2) injected animals were examined. The percentage of cells positive for Ki-67 staining was diminished in both xenograft types after treatment with C4 when compared to control treated animals (Figure 5C,D). Although the C4 treated SK-N-AS xenografts tended to have less Ki-67 staining than the saline treated controls, it did not reach statistical significance (2.07 ± 0.43% vs. 1.24 ± 0.14%, vs. C4, $P = 0.06$) (Figure 5D). However, the C4 treated SK-N-BE(2) xenografts did have a statistically significant decrease in Ki-67 staining compared to saline treated controls (3.34 ± 0.4% vs. vs. 2.33 ± 0.3%, trol C4, $P = 0.04$) (Figure 5D).

The next experiments tested the hypothesis that treatment with reduced dose C4 combined with a low-dose chemotherapeutic agent would continue to decrease tumor growth. For this study, 6-wk-old athymic nude mice were used for a tumor xenograft model and they were injected with either SK-N-AS or SK-N-BE(2) neuroblastoma cells. Doxorubicin was chosen for this experiment as it is a standard chemotherapeutic agent used clinically for neuroblastoma. Once the tumors measured approximately 100 mm^3 (Day 0), the animals (*n* = 8 mice/group) were randomized to the following groups of intraperitoneal injections for 3 wk: (1) daily vehicle (sterile normal saline); (2) daily reduced dose C4 (40 mg/kg); (3) every third day low dose doxorubicin (1 mg/kg); or (4) daily reduced dose C4 (40 mg/kg) combined with every 3 days low dose doxorubicin (1 mg/kg). Treatment with reduced dose C4 or low dose doxorubicin alone did not have a significant effect upon the growth of the SK-N-AS (Figure 6A) or SK-NBE(2) (Figure 6B) xenografts. However, the SK-N-AS xenografts treated with reduced dose C4 combined with low dose doxorubicin showed a significant decrease in growth at the completion of the study when compared to controls or either compound alone (Figure 6A). The results with combination therapy were even more marked in the SK-N-BE(2) xenografts. The animals receiving the combination reduced dose treatment of C4 and low dose doxorubicin had a significant decrease in tumor growth compared to controls or either agent alone. This decrease in tumor growth was seen early and sustained until the completion of the study (Figure 6B). These data demonstrated C4, in combination with a standard chemotherapeutic agent, was more effective at decreasing tumor growth in neuroblastoma xenografts than either agent alone.

DISCUSSION

In the current study, we have demonstrated that small molecule interruption of the FAK–VEGFR-3 interaction in neuroblastoma cells resulted in decreased cellular survival. We have also seen similar in vitro findings using a peptide to inhibit the FAK– VEGFR-3 interaction [29]. The interaction of FAK with other proteins and growth factor receptors is not unique, or limited to, VEGFR-3. In as early as 1996, FAK was found to associate with a tyrosine phosphor-ylated protein in NIH 3T3 cells after stimulation with platelet-derived growth factor [33]. Subsequently, FAK has been shown to associate with activated platelet derived growth factor receptor, epidermal growth factor receptor [34], and insulin-like growth factor-1 receptor [35]. Chen reported in 2006 that FAK directly interacts with the hepatocyte growth factor receptor c-Met, and that this interaction contributes to hepatocyte growth factor-stimulated cellular invasion [36]. FAK has also been shown to directly interact with p53, suppressing p53-induced apoptosis and inhibiting the transcriptional activity of p53 [37].

Targeting protein–protein interactions in cancers is also not a new concept, and the inhibition of protein–protein interactions with peptides has been suggested as a therapeutic strategy. Ji et al. utilized an 18-residue blocking peptide targeted to interrupt the Skp2–cyclin A interaction. These investigators found a significant decrease in cell survival in human sarcoma cells (U2OS) treated with the Skp–cyclin A interfering peptide [38]. Dasgupta et al. [39] utilized a nine amino-acid protein to disrupt the binding between Rb and Raf-1 and demonstrated decreased tumor growth and angiogenesis in a nude mouse model of human lung tumors. In efforts to find agents with higher selectivity, other investigators

have utilized small molecules to block important protein–protein interactions in cancer. Classic examples of this strategy involve the use of nutlins to disrupt the MDM2–p53 interaction [40]. Other authors have reported similar examples. Erkiznan et al. identified a small molecule that was able to disrupt the binding between the oncogenic fusion protein EWS–FLI1 and RNA helicase A. This small molecule induced apoptosis in Ewing's sarcoma cells and decreased tumor xenograft growth [41].

In this study we have shown that a small molecule, C4, will disrupt the FAK–VEGFR-3 interaction in neuroblastoma cells, leading to decreased tumor growth. This molecule was previously described by Kurenova et al. They utilized in silico docking techniques to identify potential small molecules to block the FAK–VEGFR-3 interaction, and found that this molecule decreased breast cancer cell viability and tumor growth [28]. We have demonstrated decreased neuroblastoma tumor cell survival, increased cellular apoptosis and decreased xenograft tumor growth. In our study, we noted that C4 treatment significantly decreased the phosphorylation of FAK, but did not significantly affect the phosphorylation of VEGFR-3, whereas in the previously mentioned study, the investigators noted a decrease in the phosphorylation of both kinases after C4 treatment of breast cancer cells [28]. There may be multiple explanations for these findings. The changes in VEGFR-3 phosphorylation may have been too subtle to detect with immunoblotting or may have occurred at a time point outside of our sampling. Our results may have been a function of cell line specificity, but are not necessarily a negative finding. For example, other investigators have noted similar findings, in that, the small molecule inhibition of protein–protein interactions may have more of an effect upon one protein than the other. In a study with malignant glioma cells, Manero and colleagues utilized a small molecule inhibitor of the Bcl-2 interaction with Bax. This molecule clearly disrupted the Bcl-2–Bax interaction and also decreased the expression of Bcl-2. Bax expression was not altered, but the malignant glioma cells were sensitized to radiation-induced apoptosis [42].

Amplification of the MYCN oncogene is the most important negative prognostic factor in neuroblasto ma [43,44]. Previous studies from our laboratory have shown that the MYCN oncogene functions as a transcription factor for FAK [14] and that neuroblastoma cell lines with amplification of this oncogene were more sensitive to FAK inhibition than their isogenic non-MYCN amplified counterparts [14]. We have not noted the same relation between MYCN and VEGFR-3 in neuroblastoma. Immunoblotting for VEGFR-3 in an isogenic MYCN+/MYCN– cell line did not demonstrate any change in VEGFR-3 expression with increasing MYCN expression (Supplemental Data Figure 1). The expression of this receptor does not appear to be MYCN dependent, but does vary with cell line [23,24,29]. In this study, we did utilize a *MYCN* non-amplified cell line (SK-N-AS) [45] and a *MYCN* amplified cell line [SK-N-BE(2)] [46]. In the in vitro studies, the effects of chloropyramine hydro-chloride were similar between the two cell lines. However, in the in vivo studies, the *MYCN* amplified SK-N-BE(2) xenografts were more susceptible to C4 treatment than the non-amplified SK-N-AS xeno-grafts. We believe that this finding may be explained the concept of oncogene addiction as put forth by Weinstein [47]. Weinstein proposed that the dependence upon a cell survival signal varies between cell lines of the same tumor type, and that one cell line may be more physiologically dependent upon that

factor than another cell line. In our study, the SK-N-BE (2) cell line with more FAK expression may be more physiologically dependent upon FAK than the SK-NAS cell line [14]. In the current study, C4 resulted in a more marked decrease in FAK phosphorylation in the SK-N-BE(2) cell line in vitro, and may potentially have translated into a more profound effect upon xeno-graft growth in one cell line over the other.

One of the most important findings in our study was that treatment with even low dose chloropyramine hydrochloride in combination with low dose cytotoxic chemotherapy had a significant effect upon tumor growth when compared to treatment of either agent alone. When chloropyramine hydrochloride was administered with doxorubicin, a standard neuroblastoma agent, there was a marked effect upon xenograft growth with decreased amounts of both agents. Since C4 results in decreased FAK phosphorylation, this effect may be attributed to the decreased phosphorylation of FAK. FAK has been shown to be involved in cancer chemoresistance with FAK inhibition sensitizing a number of human tumor cell types to various chemotherapy agents [48,49]. In our study, the decrease in FAK phosphorylation with C4 may have resulted in the increased sensitivity of the neuroblastoma cells to the doxorubicin, highlighting the importance of multi-faceted therapies for this tumor type.

In conclusion, the current study demonstrated that inhibition of the FAK–VEGFR-3 interaction with a small molecule, chloropyramine hydrochloride, resulted in cellular detachment, decreased cellular migration, decreased cellular viability and increased apoptosis in human neuroblastoma cell lines. In addition, this molecule, when combined with doxorubicin at low doses, resulted in decreased neuroblastoma tumor growth in a murine xenograft model. These findings are important in furthering our understanding of the regulation of neuroblastoma tumorigenesis, and may provide novel therapeutic strategies and targets for neuroblastoma and other solid tumors of childhood.

Supplementary Material

Refer to Web version on PubMed Central for supplementary material.

ACKNOWLEDGMENTS

The authors wish to thank the UAB High Resolution Imaging Facility and Shawn Williams for his outstanding technical assistance with confocal microscopy, and the UAB Neuroscience Molecular Detection Core (P30 NS47466) and Terry Lewis.

This work was supported by grants from the National Cancer Institute including [T32CA091078 to M.M.], [RO1CA65910-15 to W.G.C.] and [K08CA118178 to E.A.B.]. The content of this manuscript was solely the responsibility of the authors and does not necessarily represent the official views of the National Cancer Institute. The project described was also funded in part by grants from the Children's Neuroblastoma Cancer Foundation (E.A.B.), the Kaul Pediatric Research Institute (E.A.B.).

Abbreviations

FAK	focal adhesion kinase
VEGFR-3	vascular endothelial growth factor receptor-3

C4	chloropyramine hydrochloride
PARP	poly (ADP-ribose) polymerase
RT	room temperature

REFERENCES

1. Cotterill S, Parker L, More L, Craft A. Neuroblastoma: Changing incidence and survival in young people aged 0–24 years. A report from the North of England Young Persons' Malignant Disease Registry. Med Pediatr Oncol. 2001; 36:231–234. [PubMed: 11464892]
2. Hanks S, Polte T. Signaling through focal adhesion kinase. Bioessays. 1977; 19:137–145. [PubMed: 9046243]
3. Zachary I. Focal adhesion kinase. Int J Biochem Cell Biol. 1997; 29:929–934. [PubMed: 9375372]
4. Gabarra-Niecko V, Schaller M, Dunty J. FAK regulates biological processes important for the pathogenesis of cancer. Cancer Metastasis Rev. 2003; 22:359–374. [PubMed: 12884911]
5. Schaller M, Borgman C, Cobb B, Vines R, Reynolds A, Parsons J. pp125FAK a structurally distinctive protein-tyrosine kinase associated with focal adhesions. Proc Natl Acad Sci USA. 1992; 89:5192–5196. [PubMed: 1594631]
6. Lipinski C, Tran N, Menashi E, et al. The tyrosine kinase pyk2 promotes migration and invasion of glioma cells. Neoplasia. 2005; 7:435–445. [PubMed: 15967096]
7. Xu L, Yang X, Bradham C, et al. The focal adhesion kinase suppresses transformation associated, anchorage-independent apoptosis in human breast cancer cells. Involvement of death receptor-related signaling pathways. J Biol Chem. 2000; 275:30597–30604. [PubMed: 10899173]
8. Xu L, Yang X, Craven R, Cance W. The COOH-terminal domain of the focal adhesion kinase induces loss of adhesion and cell death in human tumor cells. Cell Growth Differ. 1998; 9:999–1005. [PubMed: 9869300]
9. Xu L, Owens L, Sturge G, et al. Attenuation of the expression of the focal adhesion kinase induces apoptosis in tumor cells. Cell Growth Differ. 1996; 7:413–418. [PubMed: 9052982]
10. Golubovskaya V, Beviglia L, Xu L, Earp Hr, Craven R, Cance W. Dual inhibition of focal adhesion kinase and epidermal growth factor receptor pathways cooperatively induces death receptor mediated apoptosis in human breast cancer cells. J Biol Chem. 2002; 277:38978–38987. [PubMed: 12167618]
11. Halder J, Landen CJ, Lutgendorf S, et al. Focal adhesion kinase silencing augments docetaxel mediated apoptosis in ovarian cancer cells. Clin Cancer Res. 2005; 11:8829–8836. [PubMed: 16361572]
12. Shi Q, Hjelmeland AB, Keir ST, et al. A novel low-molecular weight inhibitor of focal adhesion kinase, TAE226, inhibits glioma growth. Mol Carcinog. 2007; 46:488–496. [PubMed: 17219439]
13. Beierle E, Massoll N, Hartwich J, et al. Focal adhesion kinase expression in human neuroblastoma: Immunohistochemical and real-time PCR analyses. Clin Cancer Res. 2008; 14:3299–3305. [PubMed: 18519756]
14. Beierle E, Trujillo A, Nagaram A, et al. N-MYC regulates focal adhesion kinase expression in human neuroblastoma. J Biol Chem. 2007; 282:12503–12516. [PubMed: 17327229]
15. Beierle EA, Trujillo A, Nagaram A, Golubovskaya VM, Cance WG, Kurenova EV. TAE226 inhibits human neuroblastoma cell survival. Cancer Invest. 2008; 26:145–151. [PubMed: 18259944]
16. Beierle E, Ma X, Stewart J, et al. Inhibition of focal adhesion kinase decreases tumor growth in human neuroblastoma. Cell Cycle. 2010; 9:1005–1015. [PubMed: 20160475]
17. Liu X, Sun X, Wu J. Expression and significance of VEGF-C and FLT-4 in gastric cancer. World J Gastroenterol. 2004; 10:352–355. [PubMed: 14760756]
18. van Iterson V, Leidenius M, von Smitten K, Bono P, Heikkilä P. VEGF-D in association with VEGFR-3 promotes nodal metastasis in human invasive lobular breast cancer. Am J Clin Pathol. 2007; 128:759–766. [PubMed: 17951197]

19. Saintigny P, Kambouchner M, Ly M, et al. Vascular endothelial growth factor-C and its receptor VEGFR-3 in non-small-cell lung cancer: Concurrent expression in cancer cells from primary tumour and metastatic lymph node. Lung Cancer. 2007; 58:205–213. [PubMed: 17686546]
20. Herrmann E, Eltze E, Bierer S, et al. VEGF-C, VEGF-D and Flt-4 in transitional bladder cancer: Relationships to clinicopatho-logical parameters and long-term survival. Anticancer Res. 2007; 27:3127–3133. [PubMed: 17970053]
21. Kurenova EV, Hunt DL, He D, et al. Vascular endothelial growth factor receptor-3 promotes breast cancer cell proliferation, motility and survival in vitro and tumor formation in vivo. Cell Cycle. 2009; 8:2266–2280. [PubMed: 19556880]
22. Laakkonen P, Waltari M, Holopainen T, et al. Vascular endothelial growth factor receptor 3 is involved in tumor angiogenesis and growth. Cancer Res. 2007; 67:593–599. [PubMed: 17234768]
23. Beierle EA, Dai W, Langham MJ, Copeland ER, Chen M. VEGF receptors are differentially expressed by neuroblastoma cells in culture. J Pediatr Surg. 2003; 38:514–521. [PubMed: 12632379]
24. Beierle EA, Dai W, Langham MJ, Copeland E, Chen M. Expression of VEGF receptors in cocultured neuroblastoma cells. J Surg Res. 2004; 119:56–65. [PubMed: 15126083]
25. Lagodny J, Jüttner E, Kayser G, Niemeyer C, Rössler J. Lymphangiogenesis and its regulation in human neuroblastoma. Biochem Biophys Res Commun. 2007; 352:571–577. [PubMed: 17140547]
26. Rössler J, Monnet Y, Farace F, et al. The selective VEGFR 1–3 in hibitor axitinib (AG-013736) shows antitumor activity in human neuroblastoma xenografts. Int J Cancer. 2011; 128:2748–2758. [PubMed: 20715103]
27. Garces C, Kurenova E, Golubovskaya V, Cance W. Vascular endothelial growth factor receptor-3 and focal adhesion kinase bind and suppress apoptosis in breast cancer cells. Cancer Res. 2006; 66:1446–1454. [PubMed: 16452200]
28. Kurenova E, Hunt D, He D, Magis A, Ostrov D, Cance W. Small molecule chloropyramine hydrochloride (C4) targets the binding site of focal adhesion kinase and vascular endothelial growth factor receptor 3 and suppresses breast cancer growth in vivo. J Med Chem. 2009; 52:4716–4724. [PubMed: 19610651]
29. Beierle EA, Ma X, Stewart JE, Megison M, Cance WG, Kurenova EV. Inhibition of the focal adhesion kinase and vascular endothelial growth factor receptor-3 interaction leads to decreased survival in human neuroblastoma cell lines. Mol Carcinog. 2012 doi: 10.1002/mc.21969. [Epub ahead of print].
30. Manders EMM, Verbeek FJ, Aten JA. Measurement of colocalization of objects in dual-color confocal images. J Microsc. 1993; 169:375–382.
31. Frisch SM, Francis H. Disruption of epithelial cell-matrix interactions induces apoptosis. J Cell Biol. 1994; 124:619–626. [PubMed: 8106557]
32. Frisch SM, Vuori K, Ruoslahti E, Chan-Hui PY. Control of adhesion-dependent cell survival by focal adhesion kinase. J Cell Biol. 1996; 134:793–799. [PubMed: 8707856]
33. Chen HC, Guan JL. The association of focal adhesion kinase with a 200-kDa protein that is tyrosine phosphorylated in response to platelet-derived growth factor. Eur J Biochem. 1996; 235:495–500. [PubMed: 8654393]
34. Sieg DJ, Hauck CR, Ilic D, et al. FAK integrates growth-factor and integrin signals to promote cell migration. Nat Cell Biol. 2000; 2:249–256. [PubMed: 10806474]
35. Liu W, Bloom D, Cance W, Kurenova E, Golubovskaya V, Hochwald S. FAK and IGF-IR interact to provide survival signals in human pancreatic adenocarcinoma cells. Carcinogenesis. 2008; 29:1096–1107. [PubMed: 18263593]
36. Chen SY, Chen HC. Direct interaction of focal adhesion kinase (FAK) with Met is required for FAK to promote hepatocyte growth factor-induced cell invasion. Mol Cell Biol. 2006; 26:5155–5167. [PubMed: 16782899]
37. Golubovskaya VM, Finch R, Cance WG. Direct interaction of the N-terminal domain of focal adhesion kinase with the N-terminal transactivation domain of p53. J Biol Chem. 2005; 80:25008–25021. [PubMed: 15855171]

38. Ji P, Sun D, Wang H, Bauzon F, Zhu L. Disrupting Skp2–cyclin A interaction with a blocking peptide induces selective cancer cell killing. Mol Cancer Ther. 2007; 6:684–691. [PubMed: 17308064]

39. Dasgupta P, Sun J, Wang S, et al. Disruption of the Rb–Raf-1 interaction inhibits tumor growth and angiogenesis. Mol Cell Biol. 2004; 24:9527–9541. [PubMed: 15485920]

40. Vassilev LT, Vu BT, Graves B, et al. In vivo activation of the p53 pathway by small-molecule antagonists of MDM2. Science. 2004; 303:844–848. [PubMed: 14704432]

41. Erkizan HV, Kong Y, Merchant M, et al. A small molecule blocking oncogenic protein EWS–FLI1 interaction with RNA helicase A inhibits growth of Ewing's sarcoma. Nat Med. 2009; 15:750–756. [PubMed: 19584866]

42. Manero F, Gautier F, Gallenne T, et al. The small organic compound HA14-1 prevents Bcl-2 interaction with Bax to sensitize malignant glioma cells to induction of cell death. Cancer Res. 2006; 66:2757–2764. [PubMed: 16510597]

43. Brodeur GM, Seeger RC, Schwab M, Varmus HE, Bishop JM. Amplification of N-myc in untreated human neuroblastomas correlates with advanced stage disease. Science. 1984; 224:1121–1124. [PubMed: 6719137]

44. Seeger RC, Brodeur GM, Sather H, et al. Association of multiple copies of the N-myc oncogene with rapid progression of neuroblastomas. N Engl J Med. 1985; 313:1111–1116. [PubMed: 4047115]

45. Uçar K, Seeger R, Challita P, et al. Sustained cytokine production and immunophenotypic changes in human neuroblastoma cell lines transduced with a human gamma interferon vector. Cancer Gene Ther. 1995; 2:171–181. [PubMed: 8528960]

46. Nguyen T, Hocker JE, Thomas W, et al. Combined RAR alpha-and RXR-specific ligands overcome N-myc-associated retinoid resistance in neuroblastoma cells. Biochem Biophys Res Commun. 2003; 302:462–468. [PubMed: 12615055]

47. Weinstein IB. Cancer. Addiction to oncogenes—The Achilles heal of cancer. Science. 2002; 297:63–64. [PubMed: 12098689]

48. Duxbury MS, Ito H, Benoit E, Zinner MJ, Ashley SW, Whang EE. RNA interference targeting focal adhesion kinase enhances pancreatic adenocarcinoma gemcitabine chemosensitivity. Biochem Biophys Res Commun. 2003; 311:786–792. [PubMed: 14623342]

49. Chen YY, Wang ZX, Chang PA, et al. Knockdown of focal adhesion kinase reverses colon carcinoma multicellular resistance. Cancer Sci. 2009; 100:1708–1713. [PubMed: 19500106]

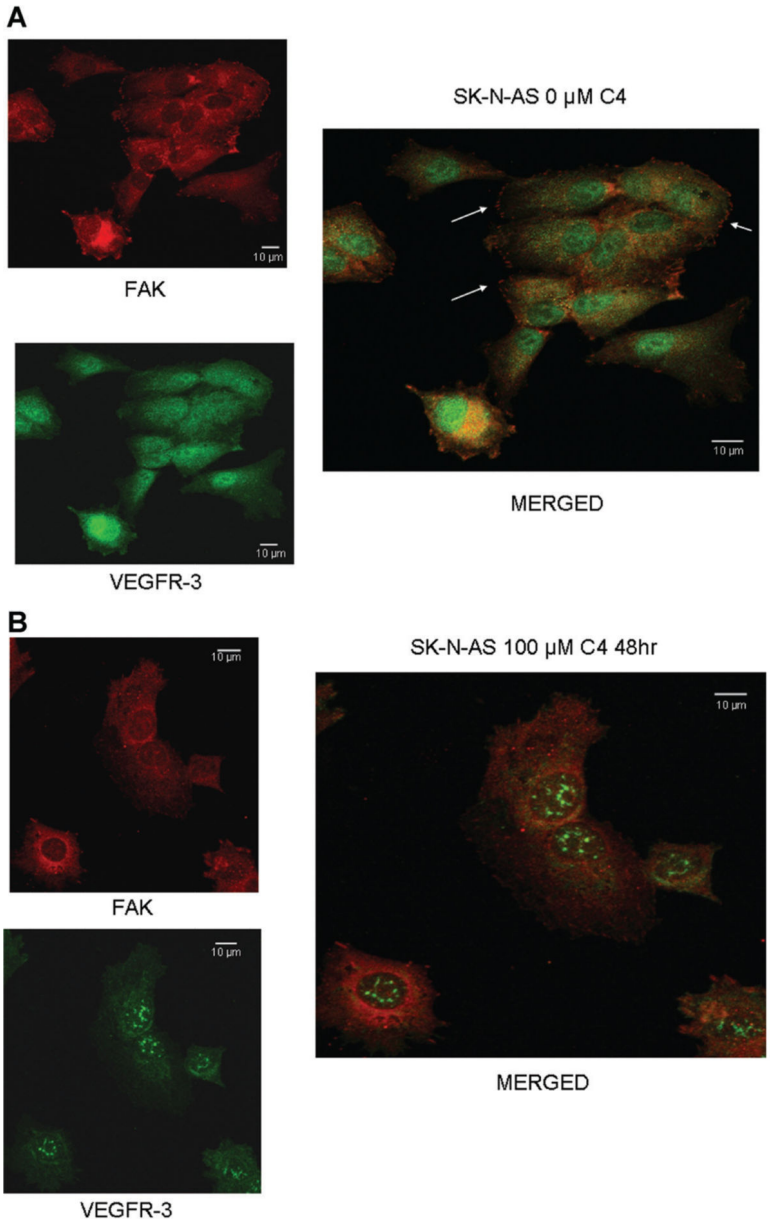

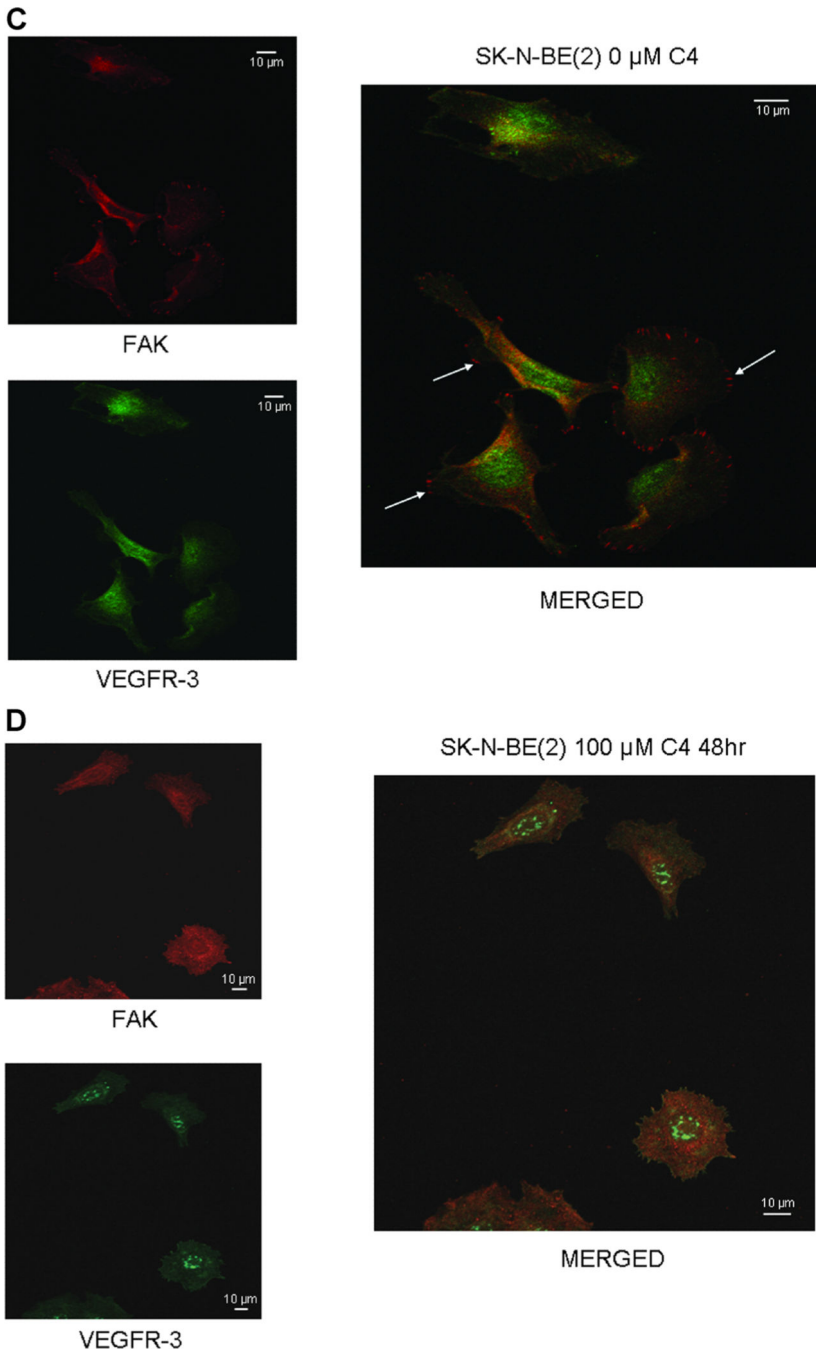

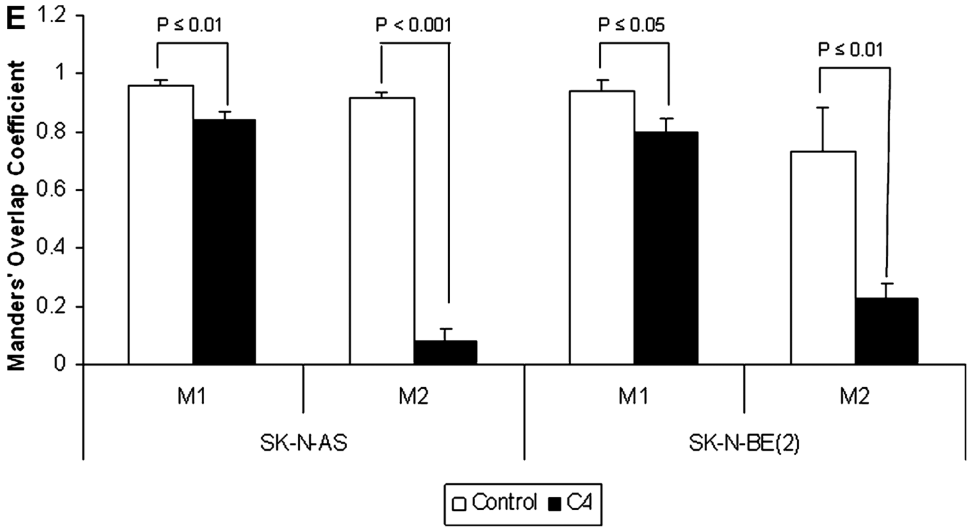

Figure 1.

C4 treatment resulted in a loss of FAK from the focal adhesions and decreased FAK-VEGFR-3 interaction. Representative photographs of immunofluorescence staining that was performed and evaluated with confocal microscopy to determine FAK and VEGFR-3 in the SK-N-AS and SK-N-BE(2) cell lines after C4 treatment for 24 h. (A) In the SK-N-AS cells, there was overlap seen between FAK and VEGFR-3, and FAK staining was seen at the focal adhesions (*right panel*, *white arrows*). (B) After C4 treatment (100 μM, 24 h) there was a loss of FAK from the focal adhesions and a decrease in the overlapped staining. (C) Overlap between FAK and VEGFR-3 was also seen in the SK-N-BE(2) cells, and FAK staining was again noted at the focal adhesions (*right panel*, *white arrows*). (D) After C4 treatment (100 μM, 24 h) there was a loss of FAK from the focal adhesions in the SK-N-BE(2) cells and a decrease in the overlapped staining. (E) Confocal images were evaluated with Meta Image Series Software to determine the amount of colocalization. Manders' overlap coefficients were calculated and compared for cells treated with C4. There was a significant difference in the overlap coefficients in the SK-N-AS cells treated with the C4 compared to controls [M1 (0.96 ± 0.02 vs. 0.84 ± 0.03, control vs. C4, $P \leq 0.01$), M2 (0.92 ± 0.02 vs. 0.08 ± 0.04, control vs. C4, cells treated with C4, there $P \leq 0.001$)]. In the SK-N-BE(2) cells treated with C4, there was also a significant decrease in the Manders' coefficients compared to controls [M1 (0.94 ± 0.04 vs. 0.80 ± 0.05, control vs. C4 $P \leq 0.05$), M2 (0.73 ± 0.15 vs. 0.23 ± 0.05, control vs. C4, $P \leq 0.01$)].

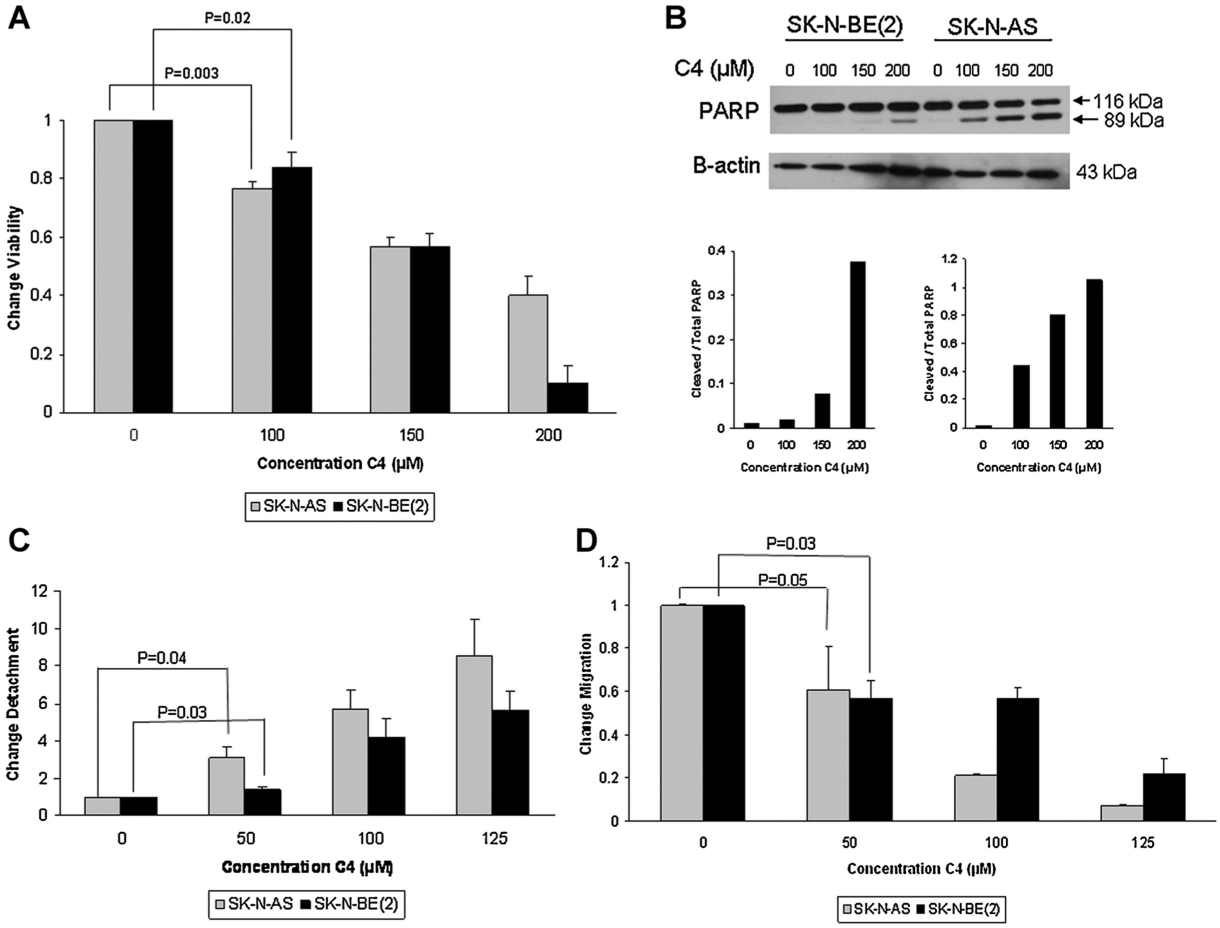

Figure 2.

C4 Decreased neuroblastoma cell viability and led to apoptosis, detachment and decreased migration. (A) SK-N-AS and SKN-BE(2) cell lines were treated with increasing concentrations of C4 for 24 h and cell viability was evaluated with alamarBlue1®® assay. Both cell lines demonstrated a significant decrease in viability after C4 treatment at 100 μM concentration. (B) Both cell lines were treated for 24 h with increasing concentrations of C4. Proteins were separated on SDS–PAGE gels and Western blotting was performed to detect cleavage of PARP, indicating apoptosis. Densitometry was used to further show the differences in cleaved PARP in both the SK-N-BE(2) (*lower left graph*) and SK-N-AS (*lower right graph*) cell lines. For densitometry, bands were normalized to β-actin and cleaved PARP compared to total PARP, further demonstrating the increased cleaved PARP following C4 treatment and indicating that the decreased survival was secondary to apoptosis. (C) SK-N-AS and SK-N-BE(2) cells were treated with C4 at increasing concentrations for 24 h. Cell detachment was determined by counting with a hemacytometer and dividing the number of detached cells by the total number of cells (attached + detached), and presented as fold change in detachment. C4 caused significant cellular detachment in both cell lines at 50 μM concentration. (D) SK-N-AS and SK-N-BE(2) cell lines were treated with increasing concentrations of C4 and allowed to migrate through a micropore insert. Migration was reported as fold change in number of cells migrating through the membrane. Cellular migration was significantly decreased in both cell lines with C4

treatment, and as seen with detachment, the effects of C4 upon migration were apparent at 50 μM concentration. The effects of C4 upon detachment and migration were seen at concentrations well below those that affected survival.

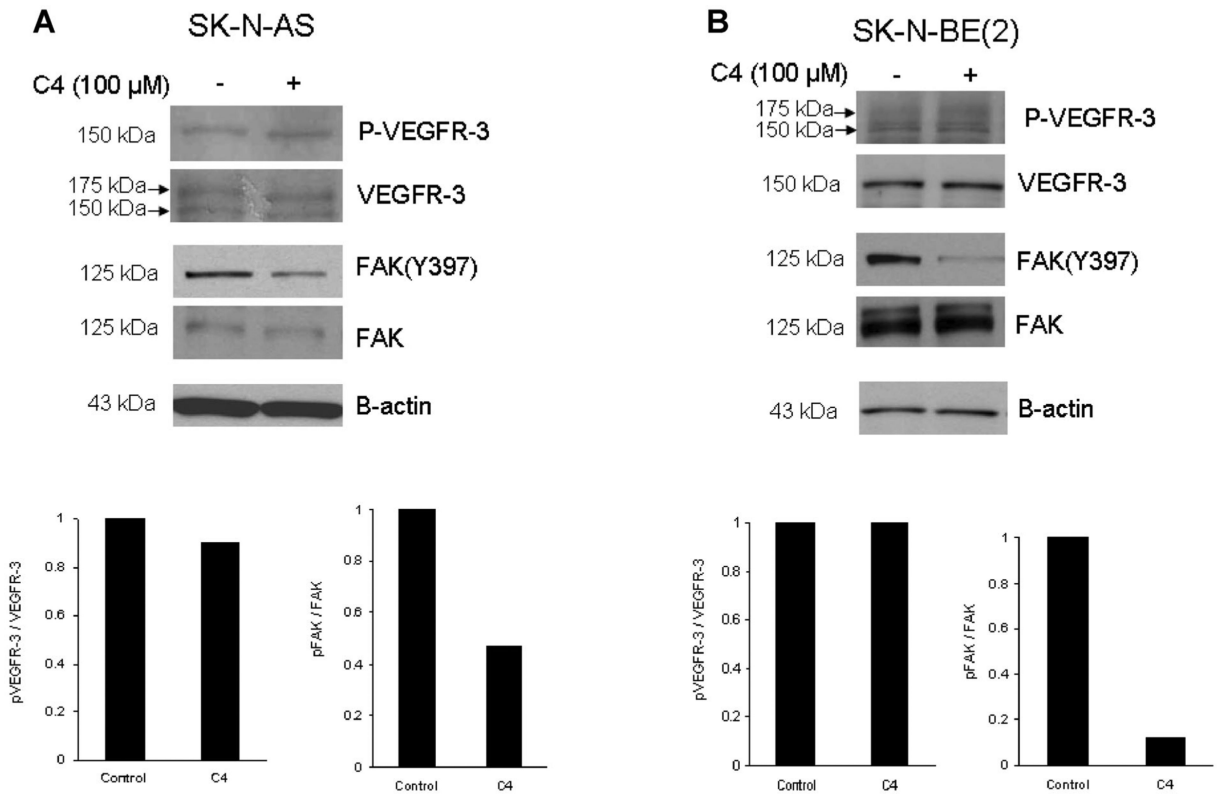

Figure 3.

C4 caused dephosphorylation of focal adhesion kinase. Immunoblotting was performed for VEGFR-3, FAK and phosphorylation of both and densitometry was used to further illustrate changes. (A) SKN-AS cells were treated with C4 at 100 μM for 24 h and were evaluated for phosphorylation of FAK and VEGFR-3. Treatment of these cells resulted in no change in the phosphorylation of Y1063/1068 VEGFR-3 (*top blot and bottom left graph*), but did decrease the phosphorylation of Y397 FAK (*top blot and bottom right graph*). (B) The SK-N-BE(2) cell line was treated with C4 at 100 μM for 24 h and phosphorylation of VEGFR-3 and FAK was examined. As seen with the SK-N-AS cells, there was no effect upon phosphorylation of VEGFR-3 (*top blot and bottom left graph*), but C4 treatment resulted in a marked decrease in Y397 FAK phosphorylation (*top blot and bottom right graph*).

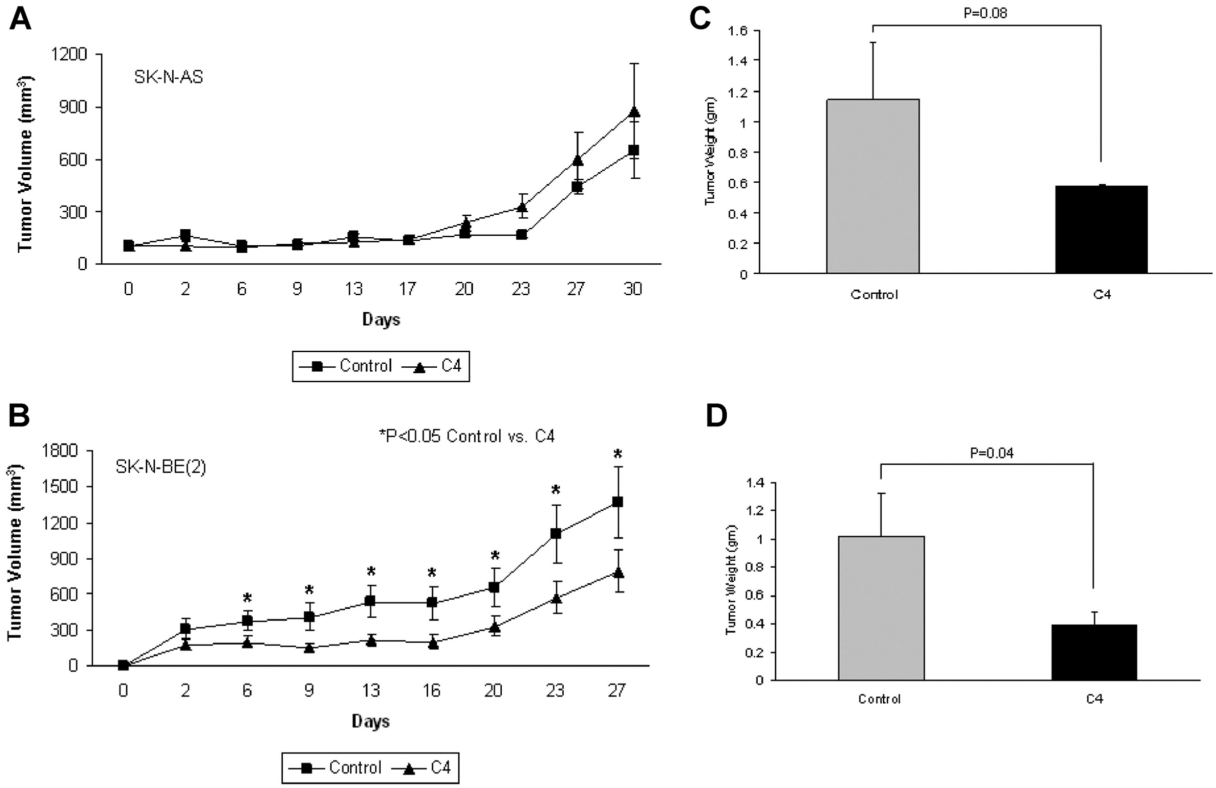

Figure 4.

C4 treatment decreased SK-N-BE(2) xenograft tumor growth. A nude mouse model was employed to study the in vivo effects of C4 treatment upon neuroblastoma xenografts. SK-N-AS and SK-N-BE(2) neuroblastoma cells were injected into the right flank of nude mice. Once the tumors became palpable (Day 0), the animals were randomized and treated daily with intraperitoneal injections of vehicle (sterile normal saline, $n = 10$) or C4 (60 mg/kg/dose, $n = 10$) and tumor volumes were measured twice weekly with calipers. (A) Treatment of the SK-N-AS xenografts with C4 decreased tumor growth, but it did not reach statistical significance. (B) C4 treatment of the SK-N-BE(2) xenografts significantly decreased the growth of the tumors. At the time of euthanasia, the tumors were harvested and weighed. In the SK-N-AS xenografts, the C4 treated tumors tended to weigh less than the saline treated controls, but did not reach statistical significance (C). In the animals with SK-N-BE(2) xenografts, the weights of the tumors treated with C4 were significantly decreased when compared to the xenografts treated with saline (D).

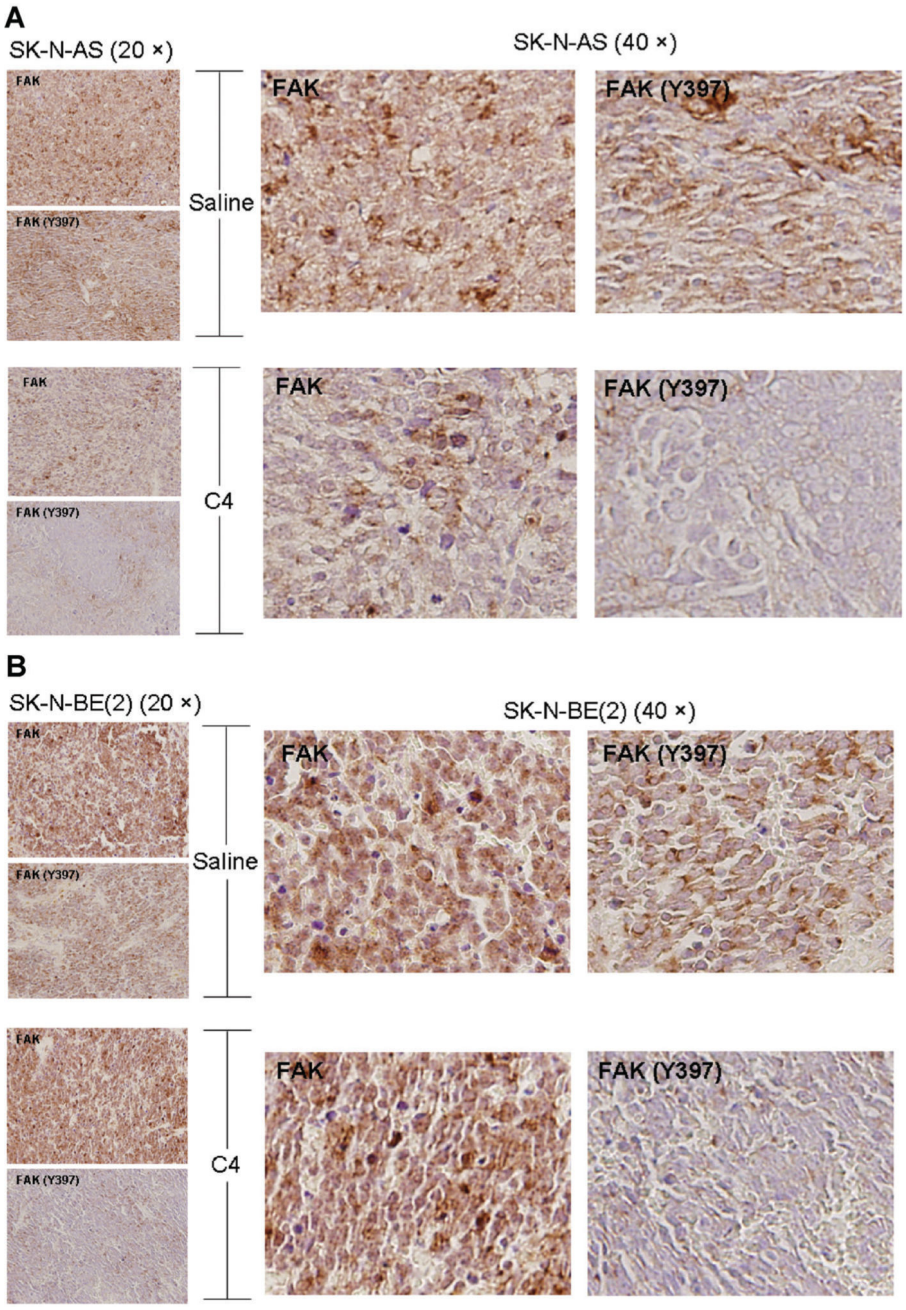

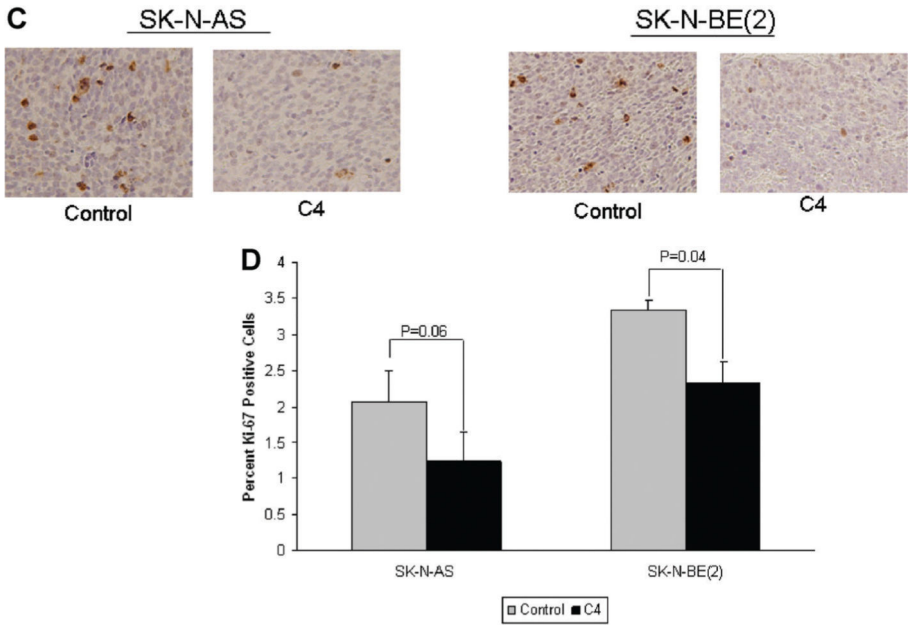

Figure 5.

C4 decreased FAK phosphorylation and proliferation in neuroblastoma xenografts. Formalin-fixed, paraffin-embedded tumor xenografts from both SK-N-AS and SK-N-BE(2) injected animals were examined. Immunohistochemical staining was performed and representative photomicrographs depicted at 20× on the left side (small boxes) and 40× on the right (large boxes). Immunohistochemistry demonstrated a decrease in the phosphorylation of FAK in both the SKN-AS (A) and SK-N-BE(2) (B) xenografts that were treated with C4. (C) Immunohistochemical staining for Ki-67 was used to detect cellular proliferation in the tumor xenograft specimens. Immunostaining for Ki-67 was diminished in both the SK-N-AS and the SK-N-BE(2) xenografts treated with C4 compared to control (saline) treated specimens. (D) Ki-67 staining was quantified with ImageJ Software and reported as percent positive staining cells per total number of cells. It was noted that the percentage of cells positive for Ki-67 staining was diminished in both xenograft types after treatment with C4. However, the C4 treated SK-N-AS xenografts were not significantly different from the tumors treated with saline. The C4 treated SK-N-BE(2) xenografts did have a statistically significant decrease in Ki-67 staining compared to saline treated controls.

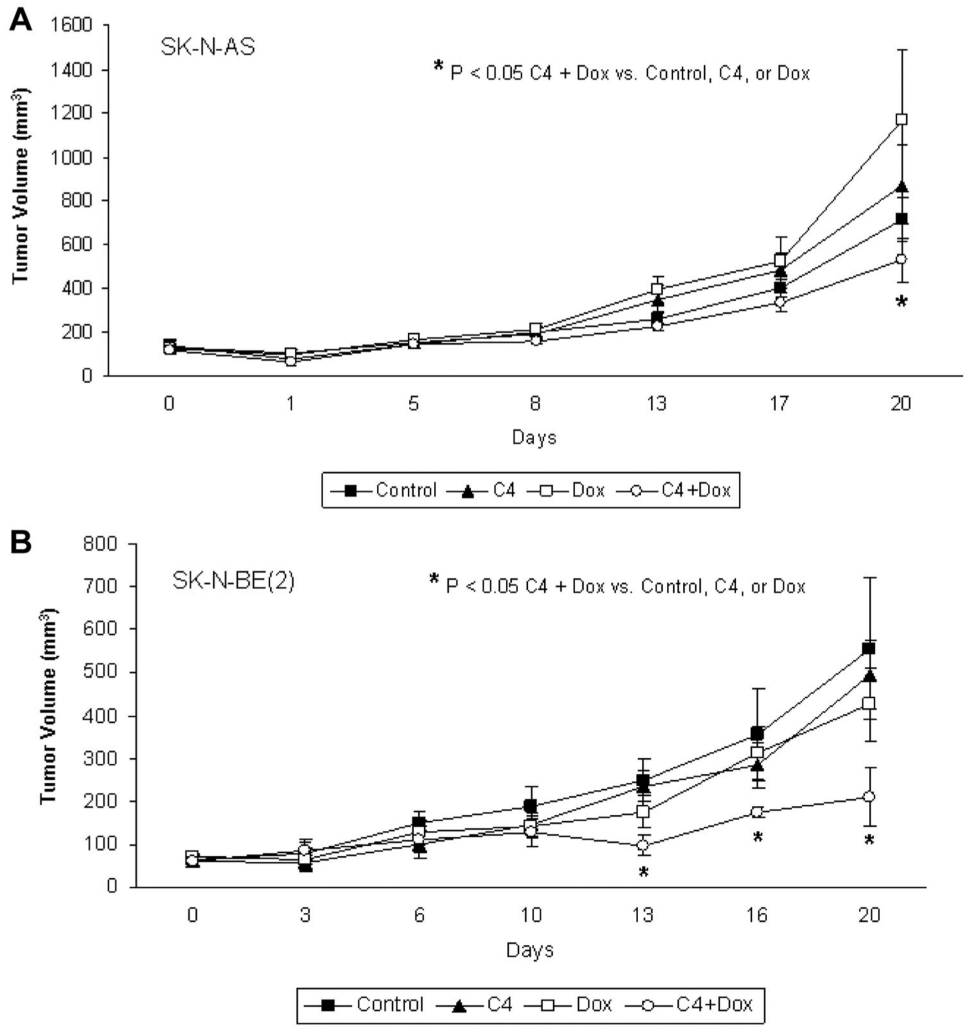

Figure 6.

C4, in combination with doxorubicin, was more effective at decreasing tumor growth in neuroblastoma xenografts than either agent alone. A nude mouse model was employed to study the in vivo effects of C4 in combination with doxorubicin. SK-N-AS and SK-N-BE(2) neuroblastoma cells were injected into the right flank of nude mice. Once the tumors measured approximately 100 mm^3 (Day 0) the animals (8 mice/group) were randomized to the following groups of intraperitoneal injections: (1) daily vehicle (sterile normal saline); (2) daily reduced dose C4 (40 mg/kg); (3) every 3 days low dose doxorubicin (1 mg/kg); or (4) daily reduced dose C4 (40 mg/kg) plus every 3 days low dose doxorubicin (1 mg/kg). Tumor volumes were measured twice weekly with calipers. (A) In the SK-N-AS xenografts, treatment with C4 or doxorubicin alone did not significantly affect tumor growth. Combination treatment with reduced dosages of both C4 and doxorubicin did result in a significant decrease in tumor growth. (B) Treatment of SK-N-BE(2) xenografts with either reduced dose C4 or low dose doxorubicin alone did not significantly reduce tumor volumes compared to controls. However, when reduced dose C4 was combined with low dose doxorubicin, there was a significant decrease in xenograft growth in the C4 + Dox group

compared to controls or either treatment alone. This decreased growth began at the second week and continued for the duration of the study.